Collapse of Parallel Folding Channels in Dihydrofolate Reductase from *Escherichia coli* by Site-Directed Mutagenesis†

Masahiro Iwakura,‡ Bryan E. Jones, Christopher J. Falzone, and C. Robert Matthews*

Department of Chemistry, Center for Biomolecular Structure and Function, and Biotechnology Institute, The Pennsylvania State University, University Park, Pennsylvania 16802

Received July 29, 1993; Revised Manuscript Received September 28, 1993®

ABSTRACT: The rate-limiting steps in the folding of dihydrofolate reductase from *Escherichia coli* have been shown to involve the conversion of a set of four intermediates to a corresponding set of native conformers via four parallel channels [Jennings *et al.* (1993) *Biochemistry 32*, 3783–3789]. Fluorescence and absorbance studies of the unfolding and refolding of the C85S/C152E double mutant at various final urea concentrations reveal two slow folding reactions, two fewer than observed in the wild-type protein. Refolding in the presence of substoichiometric levels of the inhibitor methotrexate shows that the two remaining slow reactions correspond to two parallel channels which lead to a pair of native conformers capable of binding the inhibitor. A combination of stopped-flow circular dichroism and cofactor binding studies confirms that the four parallel channels observed in the wild-type protein have collapsed into two channels in the mutant. Kinetic and equilibrium studies of the single cysteine mutants suggest that replacements of Cysteine-85 which perturb the hydrophobic core containing this side chain are responsible for the simplification of the kinetic mechanism. These results demonstrate that at least two of the parallel folding channels in dihydrofolate reductase arise when tertiary structure develops and are not dependent upon cis/trans isomerization at prolyl peptide bonds.

Protein folding reactions very often involve complex kinetic events whose time scales range from 10^{-3} to 10^{1} s (Baldwin, 1975). Prerequisites to elucidating the mechanism by which the amino acid sequence of a protein directs the folding to the native conformation include sorting out the individual phases, developing an appropriate kinetic model, and assigning the steps to specific molecular events. The complexity of protein folding reactions raises the possibility that simple linear kinetic models may not be sufficient to describe the process. Parallel folding pathways have been invoked for ribonuclease A (Schmid, 1983), staphylococcal nuclease (Evans *et al.*, 1989), hen lysozyme (Radford *et al.*, 1992), cytochrome *c* (Elöve & Roder, 1991), dihydrofolate reductase (DHFR;[1] Jennings *et al.*, 1993), and ribonuclease T1 (Mullins *et al.*, 1993).

The source of parallel folding channels from both ribonuclease A (Schmid, 1983) and staphylococcal nuclease (Evans *et al.*, 1989) has been traced to cis/trans proline isomerization in the peptide backbone (Brandts *et al.*, 1975). Although the cis isomer is favored in the native conformations of both proteins, significant portions of the unfolded proteins contain the trans isomer at the relevant Xaa–Pro peptide bonds. Folding proceeds to a near-native-like conformation containing the incorrect isomer before the final isomerization reaction produces the native conformation. Proline isomerization may also be responsible for the parallel channels in the folding of ribonuclease T1 (Mullins *et al.*, 1993). The parallel channels in cytochrome *c* have been attributed to slow ligand exchange reactions between various histidine side chains in the sequence and the heme iron (Elöve & Roder, 1991).

The parallel channels in hen lysozyme and DHFR, however, must have another explanation. Radford and co-workers (Radford *et al.*, 1992) found that the parallel channels apparent in the early stages of folding of hen lysozyme lead to the native conformation faster than would be expected if one channel required a proline isomerization step. Jennings *et al.* (1993) found that the four refolding channels leading to native or native-like conformers in DHFR are fully populated more rapidly than would be expected if the observed heterogeneity was due to proline isomerization reactions in the unfolded protein. Understanding the molecular bases of these other phenomena which can lead to heterogeneous folding populations is essential in unraveling the mechanism of folding.

A double mutant of DHFR, C85S/C152E, originally constructed to eliminate the easily oxidized cysteine residues (Iwakura *et al.*, manuscript in preparation), was found to have simplified folding kinetics. Analysis of the kinetics and comparison to the results for the wild-type protein show that the four channels observed for wild-type DHFR collapse into two channels in the double mutant. Studies of the individual cysteine mutants prove that the replacement of buried Cys-85 with the polar serine is responsible for this effect. The simplification in the folding mechanism of DHFR which can be achieved by site-directed mutagenesis enhances both the ability to extract quantitative data on folding and its interpretation.

EXPERIMENTAL PROCEDURES

Reagents. Ultrapure urea was purchased from ICN and used without further purification; fresh solutions were prepared daily. The methotrexate–agarose affinity resin was obtained

† This work was supported by NSF Grant DMB 9004707 to C.R.M.

* Address correspondence to this author at the Department of Chemistry, The Pennsylvania State University.

‡ Present address: National Institute of Bioscience and Human Technology, 1–1 Higashi, Tsukuba Science City, Ibaraki 305, Japan.

® Abstract published in *Advance ACS Abstracts*, November 15, 1993.

[1] Abbreviations: CD, circular dichroism; C85S, Cys-85 → Ser mutant; C152E, Cys-152 → Glu mutant; C85S/C152E, Cys-85 → Ser, Cys-152 → Glu double mutant; DHFR, dihydrofolate reductase; 2QF-COSY, double quantum filtered correlation spectroscopy; K_2EDTA, dipotassium ethylenediaminetetraacetic acid; MTX, methotrexate; $NADP^+$, nicotinamide adenine dinucleotide phosphate, oxidized form; NMR, nuclear magnetic resonance; UV, ultraviolet.

0006-2960/93/0432-13566$04.00/0

from Sigma and DEAE-Toyopearl 650M from Supelco. All other chemicals were reagent grade. The buffer used for all folding experiments contained 10 mM potassium phosphate, pH 7.8, 0.2 mM K_2EDTA, and 1 mM β-mercaptoethanol. The temperature was maintained at 15 °C with constant-temperature baths.

Protein Purification. Plasmid pTZDHFR12, which contains the gene encoding C85S/C152E *E. coli* DHFR, was constructed in our laboratory to remove the oxidizable cysteine residues and to introduce several unique restriction sites (M. Iwakura *et al.*, manuscript in preparation). The single mutants C85S DHFR and C152E DHFR were made from pTZDHFR12 by oligonucleotide-directed mutagenesis and cassette mutagenesis, respectively (M. Iwakura *et al.*, manuscript in preparation). DNA sequencing of the entire gene confirmed the desired mutations. All three mutants were purified from *E. coli* strain AG-1 (Stratagene) according to the method of Iwakura *et al.* (1992). From 20 g of wet cells, 100–200 mg of purified DHFR was usually obtained. DHFR was shown to be homogeneous by the observation of a single band using sodium dodecyl sulfate–polyacrylamide gel electrophoresis (Laemmli, 1970).

Protein concentration was determined by the absorbance at 280 nm using the extinction coefficient of wild-type DHFR ($\epsilon_{280} = 3.11 \times 10^4$ M^{-1} cm^{-1}; Touchette *et al.*, 1986). No detectable change in the extinction coefficient was observed for any of the mutant proteins when ϵ_{280} was determined by measuring the protein concentration with the Bradford method (Bradford, 1976). Enzymatic activity was determined by the method of Hillcoat *et al.* (1967) with the exception that the imidazole buffer was replaced with the standard buffer used for folding experiments as described above.

Folding Studies. The equilibrium unfolding reaction at 15 °C was monitored by difference UV absorbance spectroscopy at 292 nm with an AVIV 118 CX double-beam spectrophotometer (Touchette *et al.*, 1986) or by CD at 222 nm on an AVIV 62DS circular dichroism spectrometer. All samples were fully equilibrated prior to collection of the spectra. Protein concentration was 0.5 mg mL^{-1} for difference UV studies and 0.2 mg mL^{-1} for CD studies. The unfolding transition was judged to be more than 95% reversible by the recovery of the native absorption spectra following dilution from 8 M urea. The reversibility was also demonstrated by the complete recovery of the enzymatic activity after incubation in 8 M urea and dilution with buffer.

For unfolding and refolding reactions with relaxation times longer than 15 s, kinetic experiments were carried out by manual mixing methods and monitored by the change in absorbance at 292 nm on the AVIV spectrophotometer. For faster reactions, data were collected either on a Durrum 110 stopped-flow spectrophotometer or on a Bio-Logic SFM-3 stopped-flow spectrometer in the fluorescence mode. On the Durrum instrument, fluorescence was measured by exciting at 290 nm with a slit width of 5 mm. Emission intensity was monitored at wavelengths greater than 340 nm with a Corning C.S. O-52 ground-glass filter. The dead time of mixing was 18 ms when measured according to the method of Tonomura (Tonomura *et al.*, 1978). Fluorescence measurements on the Bio-Logic instrument were obtained by exciting at 290 nm with a band width of 10 nm and measuring the emission intensity at wavelengths greater than 320 nm with a ground-glass filter provided by Bio-Logic. The dead time of mixing was 5 ms when measured as above (Tonomura *et al.*, 1978). Final protein concentrations ranged from 0.1 to 0.5 mg mL^{-1}.

Ligand Binding Studies. Binding of the oxidized form of the cofactor, $NADP^+$, was monitored by quenching of tryptophan fluorescence as described by Frieden (1990) using the Bio-Logic SFM-3 stopped-flow spectrometer. Methotrexate (MTX) binding was monitored by the change in absorbance at 380 nm with the Bio-Logic instrument in the absorbance mode (Jennings *et al.*, 1993). The cuvette path length was 1 cm, and the dead time of mixing was 4 ms when measured as above. MTX concentration was determined by using a molar extinction coefficient of 2.21×10^4 M^{-1} cm^{-1} at 302 nm in 0.1 M NaOH (Stone *et al.*, 1984). The final protein concentration was 0.8 mg mL^{-1}.

Stopped-Flow CD Studies. Stopped-flow CD studies were performed on the AVIV 62DS circular dichroism spectrometer equipped with a Bio-Logic SFM-3 stopped-flow syringe system. The path length of the cuvette was 1.5 mm, and the dead time was 4 ms as measured by the method of Tonomura (Tonomura *et al.*, 1978) with the instrument in the absorbance mode. Data were acquired using the Bio-Kine software supplied by Bio-Logic, and transferred to an IBM RISC 6000 for fitting as described below. Protein concentration was typically 0.15 mg mL^{-1}.

NMR Methods. Double quantum filtered COSY (2QF-COSY) spectra (Rance *et al.*, 1983) of C85S/C152E DHFR were collected at 25 °C on a Bruker AM-500 spectrometer. The spectral widths in the F2 and F1 dimensions were 6097.6 and 6002.4 Hz, respectively. A total of 512 t_1 increments were collected, each containing 2K complex points prior to zero-filling in the F1 dimension and Fourier transformation. These data were processed on a micro VAXII or a Silicon Graphics 240 GTX using the program FTNMR written by Dr. Dennis Hare (Hare Research). Shifted sine-bell windows were used for resolution enhancement, and the 2QF-COSY spectra were referenced to H_2O at 4.76 ppm. ^1H NMR assignments were taken from previously published work (Falzone *et al.*, 1990) and from unpublished data (C. J. Falzone, in preparation). Protein concentration was typically 3 mM (53 mg mL^{-1}), and the C85S/C152E DHFR–folate complex sample also contained 4.5 mM folate. The samples were prepared by extensive dialysis in 3 mM potassium phosphate buffer (pH 6.8) which was purged with argon. Samples were lyophilized and dissolved in 450 μL of ^2H_2O containing 200 mM KCl.

Data Analysis. Equilibrium unfolding data, obtained from the difference in the extinction coefficient at 292 nm ($\Delta\epsilon_{292}$) or the ellipticity at 222 nm ($[\Theta]_{222}$), were fit to the following equation which is based on a two-state model (Santoro & Bolen, 1988):

$$Y_{obs}(\text{urea}) = [Y_N(\text{urea}) + Y_U(\text{urea})K_{app}]/(1 + K_{app}) \quad (1)$$

where Y_{obs}(urea), Y_N(urea), and Y_U(urea) are the observed $\Delta\epsilon_{292}$ or $[\Theta]_{222}$, the $\Delta\epsilon_{292}$ or $[\Theta]_{222}$ for native protein, and the $\Delta\epsilon_{292}$ or $[\Theta]_{222}$ for unfolded protein at a specified urea concentration, respectively. K_{app} represents the equilibrium ratio, [U]/[N], at any specified urea concentration. Values for Y_N(urea) and Y_U(urea) were observed to depend linearly on urea concentration in the respective base-line regions and were assumed to behave similarly in the transition region. The urea concentration dependence of K_{app} was expressed as (Schellman, 1978): $K_{app} = \exp[-(\Delta G^\circ_{H_2O} - A[\text{urea}])/RT]$. In this equation, $\Delta G^\circ_{H_2O}$ and A are the free energy difference between native and unfolded protein in the absence of urea and the cooperativity factor representing the urea dependence of the free energy change, respectively. Data obtained by different methods or from different proteins were converted

Table I: Thermodynamic Parameters for the Urea-Induced Unfolding Reaction of Wild-Type and Mutant DHFRs and Specific Activity Data

protein	ΔG_{H_2O} (kcal mol^{-1})	$-A$ [kcal mol^{-1} (M urea)$^{-1}$]	C_M (M)	activity, 15 °C (units mg^{-1})	activity, 30 °C (units mg^{-1})
wild-type[a]	6.1 ± 0.3[b]	2.0 ± 0.1	3.1 ± 0.1	13.8	60.1
C85S/C152E	4.5 ± 0.2 (UV)	2.6 ± 0.1 (UV)	1.7 ± 0.1	13.5	44.7
	4.4 ± 0.3 (CD)	2.5 ± 0.2 (CD)			
C85S	5.8 ± 0.4	2.4 ± 0.2	2.4 ± 0.1	ND[c]	ND[c]
C152E	5.8 ± 0.2	2.4 ± 0.1	2.4 ± 0.1	ND[c]	ND[c]

[a] Data taken from Touchette *et al.* (1986). [b] Errors are 95% confidence limits obtained from the nonlinear least-squares fit of the equilibrium unfolding data to eq 1. [c] Not determined.

to a form representing the apparent fraction of unfolded protein, F_{app}, as a function of urea concentration according to the equation:

$$F_{app} = [Y_{obs}(\text{urea}) - Y_N(\text{urea})]/[Y_U(\text{urea}) - Y_N(\text{urea})] \quad (2)$$

The kinetic data were fit to a sum of exponentials:

$$A(t) = \sum A_i \exp(-t/\tau_i) + A_\infty \quad (3)$$

where $A(t)$ is the total amplitude at time t, A_∞ is the amplitude at infinite time, A_i is the amplitude corresponding to the individual phase, i, at zero time, and τ_i is the associated relaxation time. Both equilibrium and kinetic data were fit by using a nonlinear least-squares fitting program, NLIN (SASA Institute Inc., Cary, NC).

RESULTS

The choice of amino acid replacements at Cys-85 and Cys-152 was based upon an inspection of the sequences found in DHFRs from other organisms (Bitar *et al.*, 1977; Gleisner *et al.*, 1974; Iwakura *et al.*, 1988) and the crystal structure of the *E. coli* protein. Cys-85 is buried in a nonpolar core near the hinge region between two structural domains (Bystroff & Kraut, 1991) and is replaced by alanine in other prokaryotes. Cys-152 has significant solvent exposure and can be replaced with larger, polar side chains such as glutamic acid, threonine, or lysine without loss of function. Therefore, Cys-85 was mutated to the small, nonpolar and polar residues glycine, alanine, or serine, and Cys-152 was mutated to serine or glutamic acid by oligonucleotide-directed mutagenesis.

The C85A/C152S and C85A/C152E double mutants have stabilities and folding kinetics which are similar to those of wild-type protein (data not shown) and are not of interest in the present study. The C85S/C152E and C85G/C152E double mutants both show measurably lower stabilities and simplified folding kinetics. The C85S/C152E DHFR was selected for further study because the presence of glycine at position 85 sufficiently destabilizes DHFR so as to leave it partially unfolded in the absence of urea (data not shown).

Equilibrium Studies. The equilibrium unfolding transitions for the C85S, C152E, C85S/C152E, and wild-type proteins are shown in Figure 1. Similar to the wild-type protein, all three mutants exhibit sigmoidal transition curves characteristic of cooperative unfolding transitions. The coincidence of the far-UV CD and near-UV absorbance transitions for the C85S/C152E double mutant (Figure 1) supports the choice of a two-state equilibrium model; coincident transitions for wild-type DHFR have been observed previously (Touchette *et al.*, 1986).

Analysis of these data according to the two-state model of Santoro and Bolen (1988; eq 1) yielded predicted transition curves which agreed very well with the observed data (Figure 1). The thermodynamic parameters derived from these fits

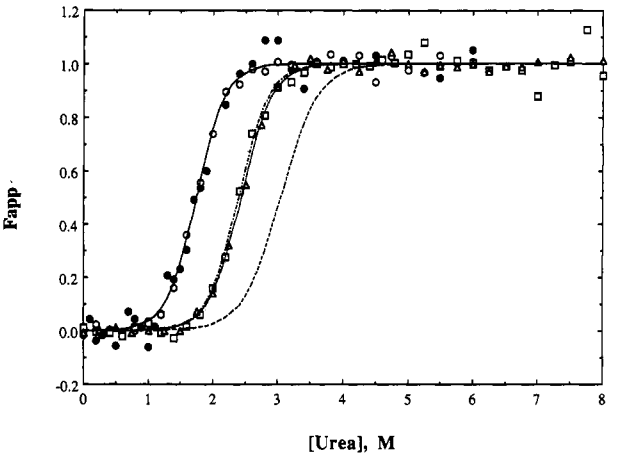

FIGURE 1: Dependence of the apparent fraction of unfolded protein, F_{app}, on the concentration of urea for C85S/C152E (○), C85S (□), and C152E (△) as observed by difference UV absorbance spectroscopy at 292 nm. The unfolding of C85S/C152E DHFR as monitored by CD ($[\Theta]_{222}$) data is also shown (●). Predicted curves based on the parameters in Table I, are shown for C85S/C152(—), C85S (- · -), C152E (···), and wild-type DHFR (- - -). The protein concentration was 0.5 mg mL^{-1} for difference UV experiments and 0.25 mg mL^{-1} for CD experiments. The buffer was 10 mM potassium phosphate (pH 7.80) containing 0.2 mM KEDTA and 1 mM β-mercaptoethanol; the temperature was maintained at 15 °C.

are listed in Table I. The apparent free energy of folding for C85S/C152E DHFR in the absence of denaturant, ($\Delta G^\circ_{H_2O}$) is 4.5 kcal mol^{-1}, substantially smaller than the 6.1 kcal mol^{-1} observed for the wild-type protein. This decrease in stability is accompanied by a decrease in the midpoint of the transition from 3.1 M urea to 1.7 M urea and an increase in the cooperativity parameter from 2.0 to 2.6 kcal mol^{-1} (M urea)$^{-1}$. The two single mutants display measurable decreases in their midpoints relative to the wild-type protein. However, the increases in their cooperativity parameters result in minimal effects on their apparent stabilities in the absence of denaturant.

To determine if these mutations cause a significant perturbation of the native conformation, the enzymatic activity of C85S/C152E DHFR was compared to that of the wild-type protein at two different temperatures. At 15 °C, the temperature at which the urea unfolding studies were done, the specific activities of both proteins were virtually identical (Table I). However, at 30 °C, the activity of the double mutant is reduced by 25%. The inferred decrease in thermal stability is consistent with the decrease in stability observed in the chemical denaturation experiments.

Kinetic Studies. The folding of DHFR has been shown to involve three distinct types of reactions. The earliest stage in folding occurs in less than 5 ms and results in the development of substantial secondary structure (Kuwajima *et al.*, 1991). The next stage occurs in the 200–300-ms time range and corresponds to the appearance of four, slowly interconverting intermediates with native-like tertiary packing between Trp-

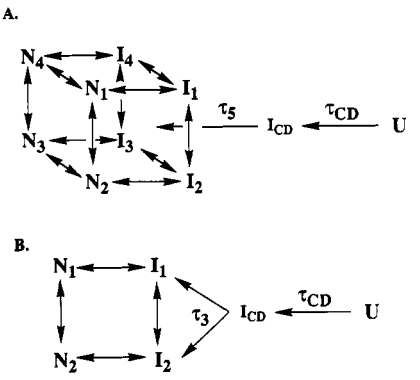

FIGURE 2: Kinetic mechanisms for the folding of wild-type DHFR (A) and C85S/C152E DHFR (B). Single-headed arrows indicate that the reactions are observed only in the refolding direction.

47 and Trp-74 (Kuwajima *et al.*, 1991). The final stage occurs in the 1–100-s time range and consists of four rate-limiting parallel channels that convert these intermediates to a set of four native conformers (Jennings *et al.*, 1993). A kinetic scheme depicting this model is shown in Figure 2A.

When the unfolding and refolding of C85S/C152E DHFR were initiated by manual mixing and monitored by the absorbance at 292 nm, single relaxation times were observed for both reactions (Figure 3). When the refolding reaction was carried out by stopped-flow techniques and monitored by fluorescence spectroscopy, three relaxation phases were observed for C85S/C152E DHFR. The fastest phase, designated the τ_3 phase, displayed an increase in tryptophan fluorescence intensity similar to the τ_5 phase of the wild-type DHFR; the slower two phases, τ_1 and τ_2, showed decreases in intensity (data not shown). The relaxation time of the slowest, τ_1, phase observed by the stopped-flow technique coincided with the single phase obtained by manual mixing (Figure 3).

A stopped-flow fluorescence study of the unfolding reaction of C85S/C152E DHFR at final urea concentrations ranging from 4 to 8 M revealed two kinetic phases. The faster phase has relaxation times in the 0.4–3-s time range, similar to the τ_2 refolding reaction of the double mutant. The small amplitude of this phase of unfolding (~10% of the signal change) and mixing artifacts at intermediate urea concentrations made it impossible to detect this phase between 2 and 6 M urea. The slower phase (~90% of the signal change) had relaxation times that closely matched the single phase detected by manual mixing UV absorbance experiments (20–90 s).

The dependencies of the observed relaxation times on the final urea concentrations are also shown in Figure 3. The log of the relaxation time of the slowest, τ_1, phase has a maximum value near 2 M urea and decreases linearly as the concentration of denaturant is either increased or decreased. This behavior is characteristic of protein folding reactions and has been observed previously (Touchette *et al.*, 1986; Matthews, 1987). The relaxation time of the intermediate, τ_2, refolding phase decreases between 1.5 and 0.4 M urea, approaching a value of 1–2 s in the absence of denaturant. Data for the τ_2 unfolding reaction are much more limited owing to mixing artifacts at urea concentrations below 7 M. However, reliable data above 7 M urea show τ_2 values around 2–3 s. Interestingly, the log of the relaxation time of the fastest, τ_3, refolding phase *decreases* linearly as the urea concentration increases from 0.4 to 1.2 M.

Under strongly folding conditions (<1 M urea), the τ_1 phase for the double mutant falls in the same time range as that for

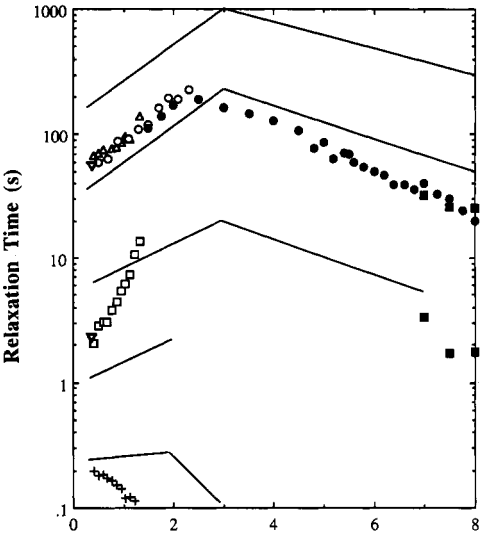

FIGURE 3: Dependence of the observed relaxation times on the final urea concentration. The slowest phase, τ_1, was measured by the UV absorption change at 292 nm on the Aviv 118 CX spectrophotometer (○, ●) and also by the fluorescence change on the Durrum stopped-flow spectrophotometer (△). The open symbols correspond to refolding and the closed symbols to unfolding. The middle, τ_2 (□), and fast, τ_3 (+), refolding phases were observed on the Durrum instrument. The relaxation times determined by stopped-flow experiments on the Bio-Logic instrument (■) for unfolding jumps from 0 M to the indicated urea concentration are also plotted. Relaxation times observed by MTX binding during refolding are also shown (▽). Solid lines indicate the approximate relaxation times (τ_1, the slowest, through τ_5, the fastest) observed for wild-type DHFR (Jennings *et al.*, 1993). Refolding jumps were done by diluting a protein/4.5 M urea solution with buffer and urea to the desired final urea concentration; unfolding jumps were accomplished by diluting a protein solution with urea and buffer to the desired final urea concentration. Final protein concentrations were 0.5 mg mL^{-1} for manual mixing experiments and 0.2 mg mL^{-1} for stopped-flow experiments; solvent conditions were identical to those described in Figure 1.

the τ_2 phase in the wild-type protein (Figure 3, solid lines). The τ_2 phase in the double mutant approaches that for the τ_4 phase for wild-type DHFR, and the fastest, τ_3, phase occurs in a similar time range as the τ_5 phase observed for wild-type DHFR.

Parallel versus Sequential Folding Mechanism for C85S/C152E DHFR. MTX, a tight binding, competitive inhibitor of DHFR (K_d < 1 nM; Appleman *et al.*, 1988), has been useful in choosing between parallel or sequential folding mechanisms in the wild-type protein (Jennings *et al.*, 1993). Absorbance changes at 380 nm, where the difference spectrum between bound and free MTX has a maximum, can be used to monitor inhibitor binding without any contributions from the protein (Touchette *et al.*, 1986).

When the refolding of C85S/C152E DHFR was performed in the presence of excess MTX (Figure 4), a lag phase followed by two slow binding phases was observed. These two phases have relaxation times (2.1 and 50.7 s) which coincide precisely with those of the τ_1 and τ_2 phases detected by refolding experiments without MTX (Figure 3); the relative amplitudes were 78% and 22%. The lag phase in the first 200 ms (Figure 4, inset) shows that the intermediate formed by the τ_3 reaction cannot bind MTX. This behavior is similar to that observed for the intermediates formed in the τ_5 phase for the wild-type protein (Jennings *et al.*, 1993).

Refolding C85S/C152E DHFR in the presence of a substoichiometric amount of MTX leads to a selective loss of

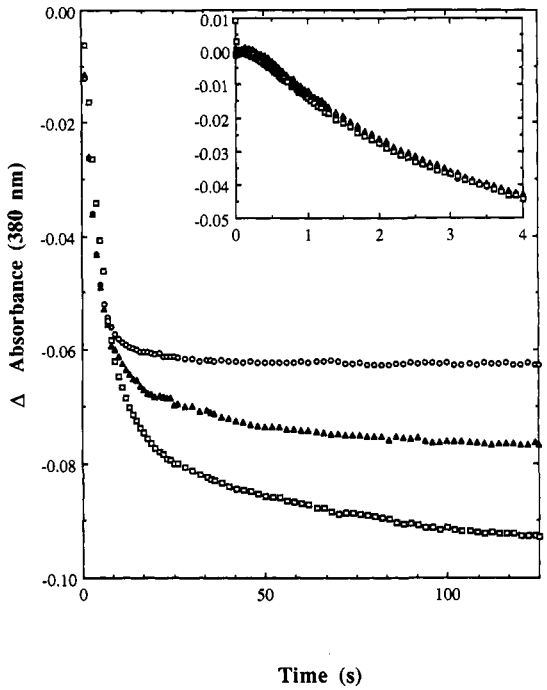

FIGURE 4: Change in the absorbance at 380 nm during the refolding reaction of C85S/C152E DHFR from 4.5 M urea to 0.45 M urea in the presence of various amounts of MTX as measured on the Bio-Logic SFM-3 stopped-flow instrument. The MTX/C85S/C152E DHFR ratios are 1.1/1 (□), 0.8/1 (▲), and 0.7/1 (○). The inset shows the first 5 s of these reactions. The final protein concentration was 0.8 mg mL^{-1} (45 μM), and the MTX concentration was varied; solvent conditions were as described in Figure 1.

Table II: Amplitudes[a] and Relaxation Times for the Refolding[b] of C85S/C152E DHFR[c] Monitored by Tryptophan Fluorescence in the Presence and Absence of NADP$^+$

addition	A_3 (V)	τ_3 (s)	A_2 (V)	τ_2 (s)	A_1 (V)	τ_1 (s)
control	−0.86	0.205	0.85	2.22	0.69	59.9
9.1 μM NADP$^+$	−0.84	0.193	0.79	2.23	1.97	59.2
91 μM NADP$^+$	−0.83	0.189	0.78	2.20	2.39	67.1

[a] Amplitude changes are in volts with a negative value reflecting an increase in the observed signal. [b] Refolding jumps were done from 4.5 to 0.41 M urea at 15 °C in the standard 10 mM potassium phosphate buffer, pH 7.8. [c] The final protein concentration was 6.8 μM.

the slow binding phase. At a ratio of 0.7 mol of MTX/mol of DHFR, no further changes in the absorbance at 380 nm occur after 30 s (Figure 4). These data are consistent with the predictions of parallel folding channels. At substoichiometric concentrations of MTX, the faster folding native conformers bind the available inhibitor and deplete the MTX supply. The decreased supply of MTX selectively reduces the signal change due to the binding of the inhibitor to the slower folding species (Jennings *et al.*, 1993).

Refolding Kinetics in the Presence of the Oxidized Form of the Coenzyme NADP$^+$. Another probe that can be used to discriminate among the folding channels is the quenching of tryptophan fluorescence caused by the binding of the oxidized form of the cofactor NADP$^+$. The amplitude of only a single refolding phase for wild-type DHFR (the τ_2 phase) is increased in the presence of NADP$^+$, indicating that binding is selective for this particular channel (Jennings *et al.*, 1993).

When the same experiment is performed with C85S/C152E DHFR, only the amplitude of the slowest, τ_1, phase is markedly increased in the presence of NADP$^+$ (Table II). Therefore, this channel behaves in a fashion similar to the τ_2 channel in the wild-type protein. Because the products of these channels bind both MTX and NADP$^+$, it is likely that they represent the formation of the active enzyme in both the wild-type and double mutant DHFR.

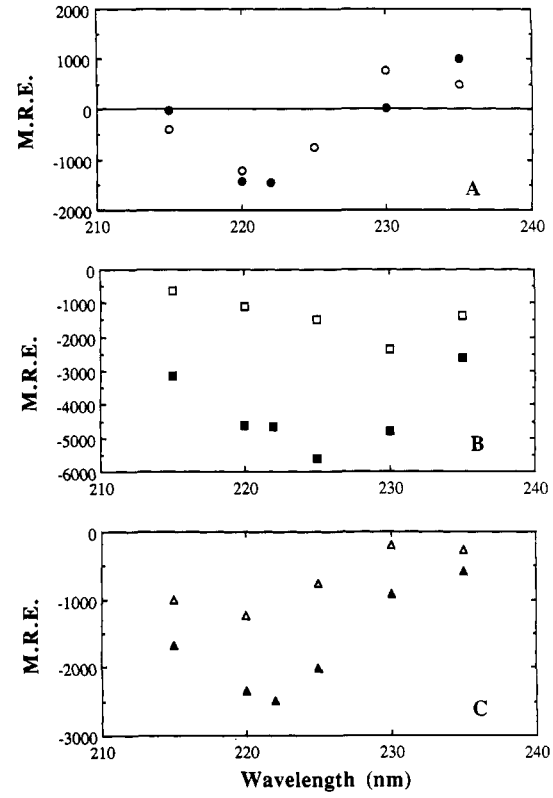

FIGURE 5: Kinetic CD difference spectra obtained from stopped-flow CD experiments. The units (MRE) are in degrees centimeter squared per decimole. The signal changes for τ_3 (A), τ_2 (B), and τ_1 (C) for a refolding jump from 4.5 M urea to 0.5 M urea are plotted as a function of wavelength (closed symbols). For comparison, similar data for the wild-type τ_5 (A), τ_4 (B), and τ_2 (C) are plotted as open symbols [taken from Kuwajima et al. (1991)]. The observed magnitude difference in the two slower phases for the mutant (panels B and C), as compared to the data for wild-type DHFR, is due to differing amounts of protein folding through each of the two channels. The final protein concentration was 0.15 mg mL^{-1}; the solvent was identical to that described in Figure 1.

Stopped-Flow Circular Dichroism Study. Another means of discriminating between folding channels in DHFR is by examining the wavelength dependence of the amplitudes of the various refolding phases detected by far-UV CD spectroscopy. The refolding of wild-type DHFR monitored by the stopped-flow far-UV CD technique displays the same five kinetic phases detected by absorbance and fluorescence spectroscopies (Kuwajima *et al.*, 1991). The amplitudes of these phases as a function of detection wavelength show distinctive patterns which reflect the formation (or disruption) of secondary and tertiary structure. The amplitudes of the slower pair of relaxation processes, the τ_1 and τ_2 phases, have similar patterns and were different from those of the faster pair of processes, the τ_3 and τ_4 phases. The τ_1 and τ_2 pair of channels exhibit minima near 220 nm, and the τ_3 and τ_4 pair exhibit minima between 225 and 230 nm. Representative kinetic difference spectra for the τ_5, τ_4, and τ_2 phases of the wild-type protein are shown in Figure 5A–C (Kuwajima et al., 1991). Thus, the measurement of the wavelength dependence of the far-UV ellipticity of the two remaining slow phases in C85S/C152E DHFR can be used to clarify which of the three types of phases in the wild-type protein persist.

The kinetic difference spectra for each of the three refolding phases observed for C85S/C152E DHFR are also shown in

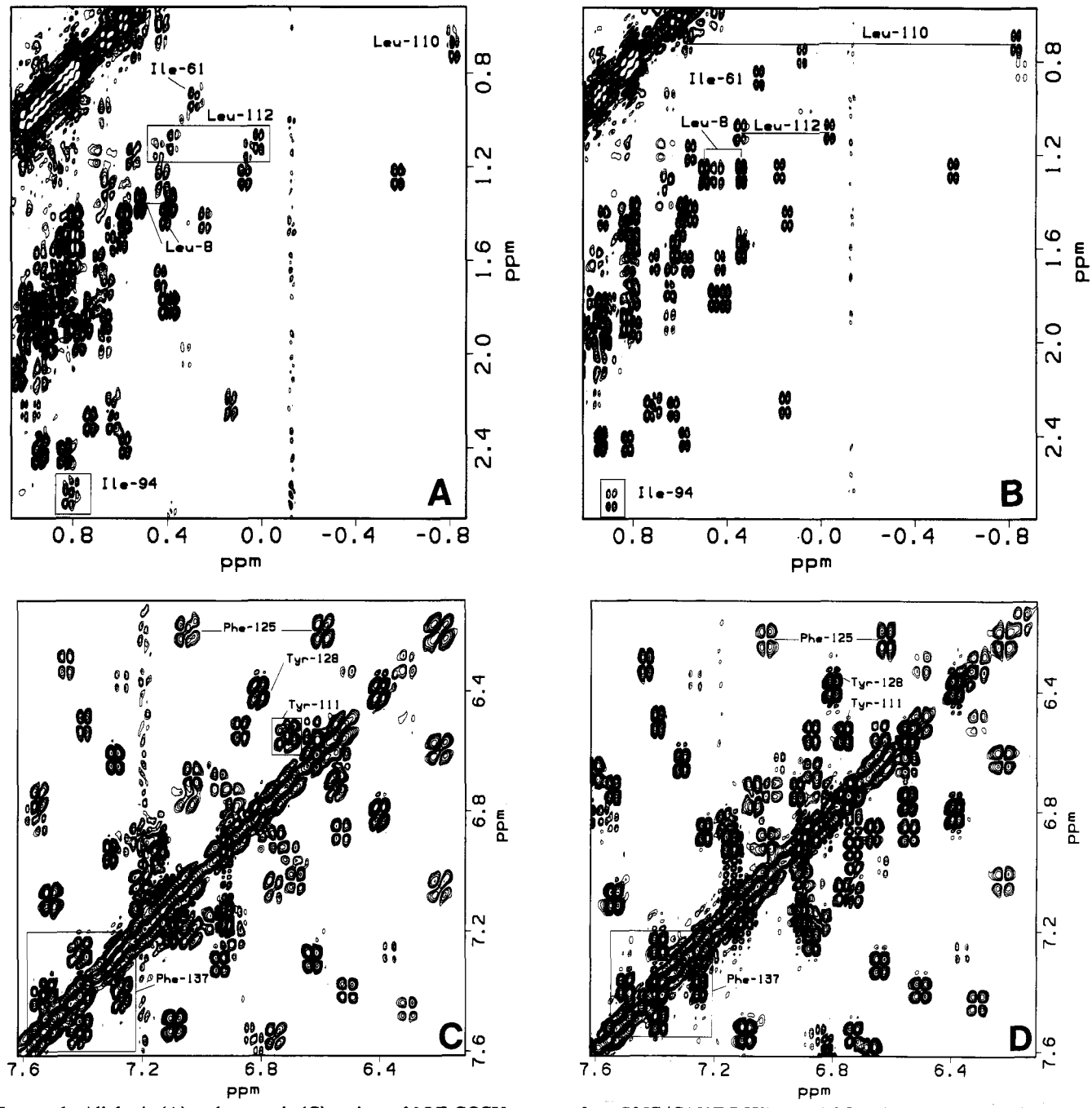

FIGURE 6: Aliphatic (A) and aromatic (C) regions of 2QF-COSY spectra of apoC85S/C152E DHFR at 25 °C. The same regions of spectra of the C85S/C152E DHFR/folate complex are also shown (B and D). Assignments of residues are based on spectra of wild-type DHFR (Falzone *et al.*, 1990; C. J. Falzone, unpublished results). The protein concentration was 3 mM (53 mg mL^{-1}), and the DHFR/folate complex also contained 4.5 mM folate. The samples were prepared by extensive dialysis in 3 mM potassium phosphate buffer (pH 6.8) purged with argon, followed by lyophilization. Lyophilized samples were dissolved in 450 μL of ^2H_2O containing 200 mM KCl.

Figure 5. The amplitude of the τ_3 phase displays a minimum near 222 nm and a crossover to positive values at 230 nm (Figure 5A). This behavior is similar to that observed for the τ_5 phase in the folding of wild-type DHFR (Kuwajima *et al.*, 1991) and reflects the native-like tertiary packing between the Trp-47 and Trp-74 side chains. The minimum near 225 nm observed for τ_2 (Figure 5B) is similar to that observed for τ_3 and τ_4 in the wild-type protein, and the minimum near 220 nm for τ_1 (Figure 5C) is similar to that observed for τ_1 and τ_2 (Kuwajima *et al.*, 1991). These results confirm the early appearance of tertiary packing between Trp-47 and Trp-74 and demonstrate that the slower channel in the double mutant resembles the τ_1 and τ_2 pair in wild-type DHFR and the faster channel resembles the τ_3 and τ_4 pair of channels in the wild-type protein.

Multiple Native Conformers in C85S/C152E DHFR. The pair of unfolding reactions observed for C85S/C152E DHFR implies that, similar to the wild-type protein, two stable native conformers exist. To test this hypothesis, a two-dimensional NMR analysis of C85S/C152E DHFR was performed. Wild-type DHFR is known to display a doubling of a number of cross-peaks, consistent with the presence of two slowly interconverting species (Falzone *et al.*, 1991). Figure 6 shows the aliphatic (A) and aromatic (C) regions of a 2QF-COSY spectrum of apo-C85S/C152E DHFR. Similar to the wild-type protein, a number of resonances show clear doubling; Ile-94, Leu-112, Tyr-111, and Phe-137. Many others, including Ile-61, Phe-125, and Tyr-128, display broadening or are too weak to detect, especially in the fingerprint region (data not shown). The doubling of the cross-peaks associated

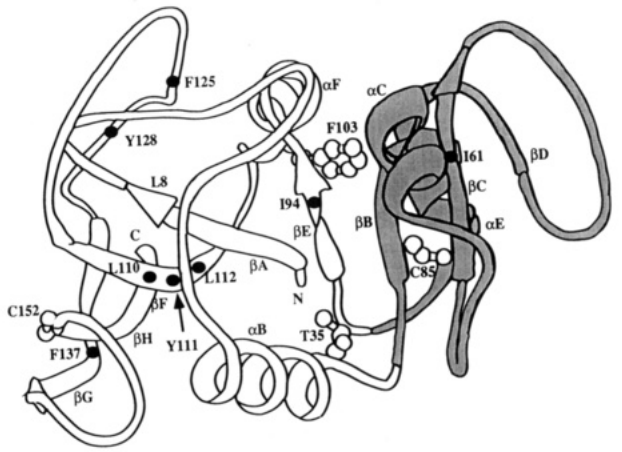

FIGURE 7: Ribbon diagram of the backbone of DHFR (Bolin *et al.*, 1982), showing the side chains of Thr-35, Cys-85, Phe-103, and Cys-152. The adenine binding domain (Bystroff *et al.*, 1990) is shaded, and the various elements of secondary structure are indicated. Filled circles indicate the positions of residues highlighted in Figure 6.

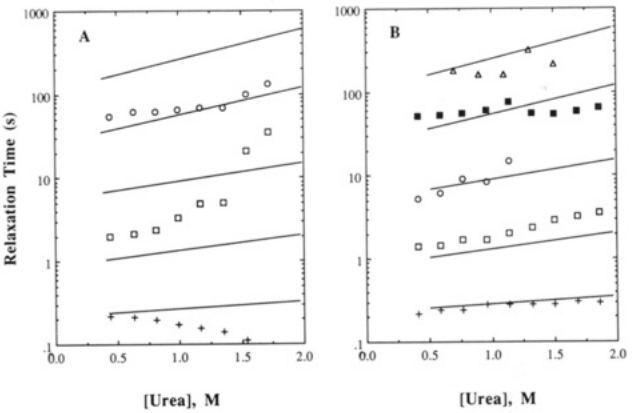

FIGURE 8: Relaxation times observed for C85S DHFR (A) and C152E DHFR (B) under refolding conditions. (A) Relaxation times were determined by stopped-flow fluorescence on the Durrum instrument for the fastest (τ_3, +) and intermediate (τ_2, □) phases. The slowest phase (τ_1, ○) was measured by the UV absorption at 292 nm of the Aviv 118 CX spectrometer; symbols refer to relaxation times for refolding jumps from 4.5 M urea to the desired final urea concentration. (B) Relaxation times were determined on the Durrum instrument for the τ_5 (+), τ_4 (□), τ_3 (○), and τ_2 (■) phases. Relaxation times for the slowest, τ_1, phase (△) were measured on the Aviv spectrometer, as described above. Solvent conditions were as described in Figure 1.

with residues in different regions of the protein (Figure 7) supports the conclusion that two slowly interconverting conformers also exist in C85S/C152E DHFR under native conditions.

For comparison, the corresponding regions of the spectrum obtained from the complex of C85S/C152E DHFR with folate are shown (Figure 6B,D). For all of the examples highlighted, the addition of folate results in single resonances and, in general, a much cleaner spectrum. These data demonstrate that, similar to the wild-type protein, one form of C85S/C152E DHFR predominates in the presence of folate (Falzone *et al.*, 1990). This conformer presumably corresponds to the material folding through the τ_1 channel in C85S/C152E DHFR (which binds $NADP^+$; Table II).

Assignment to a Specific Cysteine Residue. The assignment of the simplification in the folding mechanism to one or both of the mutations was made by examining the refolding reactions of the single mutants. Only three refolding phases were observed by stopped-flow fluorescence and manual mixing techniques in the refolding of the C85S mutant DHFR (Figure 8A). The fastest, τ_3, phase reflects an increase in fluorescence intensity, while the slower τ_1 and τ_2 phases reflect decreases in fluorescence intensity. Similar to wild-type DHFR, the refolding of C152E DHFR exhibited five phases (Figure 8B). The fastest phase displays an increase in fluorescence intensity, and the four slower phases display decreases in fluorescence intensity. These data demonstrate that the simplified kinetic response in C85S/C152E DHFR is due to the substitution with serine at position 85.

DISCUSSION

Several lines of evidence suggest that the τ_1 and τ_2 folding channels in the wild-type DHFR coalesce into the τ_1 channel for the C85S/C152E DHFR and that the τ_3 and τ_4 channels coalesce into the τ_2 channel in the double mutant:

(1) The sum of the τ_1 and τ_2 amplitudes for MTX binding to wild-type DHFR, 19%, agrees very well with that for the τ_1 amplitude in the mutant DHFR, 22%. As expected for normalized amplitudes, the sum of the τ_3 and τ_4 amplitudes in wild-type protein, 81%, also agrees closely with that for the τ_2 amplitude in the mutant protein, 78%.

(2) The CD kinetic difference spectrum of the τ_1 channel in the mutant DHFR matches those for the τ_1 and τ_2 channels in wild-type DHFR. Also, the spectrum for the τ_2 channel in the mutant is similar to those for the τ_3 and τ_4 channels in wild-type protein.

(3) $NADP^+$ uniquely binds to the product of the τ_2 phase in the folding of wild-type DHFR. The oxidized cofactor only binds to the product of the τ_1 phase in the folding of the double mutant. Apparently, the coalescence of the τ_1 and τ_2 channels of the wild-type protein into the τ_1 channel of the mutant results in active enzyme properties for this channel.

A kinetic folding model for C85S/C152E DHFR is shown in Figure 2B. The development of substantial ellipticity in the burst phase of folding (<5 ms) for the double mutant (data not shown) demonstrates that this protein retains the initial stage, i.e., τ_{CD}, displayed by wild-type DHFR (Kuwajima *et al.*, 1991). This early intermediate, I_{CD}, then folds in the 100–200-ms time range into a pair of subsequent species, I_1 and I_2, in which Trp-47 and Trp-74 achieve a native-like packing. The evidence for this specific tertiary structure is the kinetic difference spectrum of the τ_3 phase (Figure 5A). This spectrum is identical to that for the τ_5 phase in wild-type DHFR where mutational analysis has shown that the spectrum arises from exciton coupling between these two chromophores (Kuwajima et al., 1991). This pair of intermediates then fold via the τ_1 and τ_2 channels into a corresponding set of native conformers, N_1 and N_2. Both N_1 and N_2 are sufficiently native-like to bind to MTX, but only N_1 can also bind $NADP^+$. The capability of binding both active-site inhibitor and oxidized cofactor suggests that N_1 is the active enzyme form in the double mutant.

Examination of the dependence of the unfolding and refolding relaxation times on the final denaturant concentration for C85S/C152E DHFR (Figure 3) reveals two significant differences when compared to wild-type protein. First, the slope of the τ_2 phase in refolding is considerably increased over those of the τ_3 and τ_4 phases for the wild-type protein. It has been argued that the slopes of such plots are directly proportional to the difference in the interaction energy of the chemical denaturant with a kinetic species in a folding mechanism and the transition state which follows it (Chen *et al.*, 1989). If this difference is attributed to the change in the solvent exposure of side-chain and backbone atoms for the

activation process (Kuwajima *et al.*, 1989), the increased slope implies a greater change between I_2 and the rate-limiting transition state for the double mutant compared to wild-type DHFR. Inspection of the data for the single cysteine mutants (Figure 8) reveals that this slope effect is due to the C85S mutation. One mechanism by which a single amino acid replacement could cause such a dramatic change in solvent exposure is if I_2 were to be destabilized by this mutation. The effect on the kinetic mechanism would be to involve folding from either I_{CD} or perhaps U directly to N_2. Because either I_{CD} or U is expected to have a greater solvent exposure for backbone and side-chain groups than I_2, the slope of the kinetic plot would increase as observed. As is discussed below, I_2 does appear to be destabilized by the C85S mutation. The absence of a similar effect for the τ_1 refolding relaxation time shows that the side chain at position 85 has a different environment in the I_1 intermediate and transition state than it does in the τ_2 channel for the double mutant.

The second significant difference in the dependence of the relaxation times on the denaturant concentration for the C85S/C152E mutant is the behavior of the τ_3 refolding phase. Unlike wild-type DHFR in which the equivalent reaction, τ_5, has an inverted V or chevron shape, τ_3 for the mutant decreases monotonically as the urea concentration increases (Figure 3). Examination of the behavior of the single cysteine mutants (Figure 7) shows that this effect is solely due to the C85S mutation.

The simplest explanation for this effect is that the replacement of cysteine with serine destabilizes one or both of the products of τ_3 reaction, i.e., I_1 and/or I_2. As a result, the relaxation time primarily reflects the unfolding rate constants for the $I_1 \rightarrow I_{CD}$ and/or $I_2 \rightarrow I_{CD}$ reactions (Matthews, 1987). Unfolding relaxation times decrease with increasing denaturant concentration (Tanford, 1968), reflecting the shift of folded to unfolded conformations. In effect, the inverted V has shifted to lower urea concentration, thus making only the right-hand side observable in refolding experiments. As noted above, it is possible that the I_2 species is indeed destabilized by the C85S mutation but the I_1 species is not. The observed monotonic decrease in relaxation time for the τ_3 phase probably reflects the predominance of the τ_2 refolding phase over the τ_1 phase (4-fold more MTX binds to the product of the τ_2 reaction as for that of the τ_1 reaction).

Weissman and Kim (1991) have observed the acceleration of a disulfide bond rearrangement reaction in pancreatic trypsin inhibitor at increasing urea concentration. These investigators attributed this result to the destabilization of native-like structure in a two-disulfide intermediate. Kiefhaber et al. (1992) have detected a similar effect on a slow-folding step in ribonuclease T1 and concluded that specific tertiary interactions in partially-folded intermediates can serve to decrease the rate of folding. These several examples suggest that folding intermediates may act as transient kinetic traps during the folding reaction.

The observation of four parallel folding channels in wild-type DHFR and only two when Cys-85 is replaced with serine is most easily explained by assuming that there are two independent conformational situations which can exist in either of two distinct forms. Although cis/trans isomerization at Xaa–Pro peptide bonds (Brandts *et al.*, 1975) is an attractive candidate, a previous study has shown that this is not likely to be the explanation for DHFR (Jennings *et al.*, 1993). The results of the present study, which involves amino acid replacements that are not at or adjacent to proline residues, support this conclusion.

Studies on the single cysteine mutants (Figure 8) demonstrate that it is the replacement of Cys-85 with serine that is responsible for the simplification of the folding mechanism of DHFR. Although the apparent stability in the absence of denaturant for the C85S mutant is very similar to wild-type protein, the midpoint of the urea-induced unfolding transition is substantially lower in the mutant (Table I). These contradictory results may reflect on the role of the cooperativity parameter, A, in determining the stability (Alonso & Dill, 1991) or on the validity of assuming that the free energy depends linearly on the denaturant concentration (Schellman, 1978). Whatever the explanation, the introduction of serine at position 85 clearly perturbs the equilibrium as well as the kinetic properties of DHFR. Results from studies of other mutations at Cys-85 are consistent with the correlation between the perturbation on stability and the simplification of the folding kinetics. Replacement of Cys-85 with alanine has no measurable effect on the stability and does not affect the kinetic response, whereas replacement with glycine destabilizes the protein and also reduces the number of kinetic phases observed (data not shown).

Inspection of the crystal structure of apoDHFR (Figure 7; Bystroff & Kraut, 1991) shows that Cys-85 is part of a hydrophobic core which defines a hinge between two structural domains. Perhaps this hinge and the two domains which it links can adopt either of two different conformations at this stage of the folding reaction. The selective destabilization of one of these conformers in the Cys-85 mutant could account for the loss of a pair of channels. Replacement of another residue near the hinge region, Thr-35 (Jennings and Matthews, unpublished results), and one at the domain interface, Phe-103 (Finn and Matthews, unpublished results), also causes the loss of two of the four slow-folding phases. Taken together, these findings support the view that at least one source of folding channels in DHFR is alternative domain orientations.

A possible explanation of the remaining pair of channels in C85S/C152E DHFR is suggested by the results of NMR and X-ray studies. The 2QF-COSY spectra of both the wild-type protein [Figures 1, 2, and 5 in Falzone *et al.* (1991)] and C85S/C152E DHFRs (Figure 6) show a doubling of a number of side-chain cross-peaks (with MTX bound or as the apoprotein). In both the wild-type and double mutant DHFRs, the majority of residues with doubled resonances reside in the β-sheet [Figure 6 in Falzone *et al.* (1991)]. Examination of the crystal structure (Bolin *et al.*, 1982; Bystroff *et al.*, 1990; Bystroff & Kraut, 1991) suggests two possible explanations for these effects: bulges in the β-sheet or a cis peptide bond. The β-sheet in DHFR has three distortions or bulges at positions 95, 109, and 137 (Bolin *et al.*, 1982). Perhaps one of these bulges is absent in the alternative conformer. The requirement to change the register of the strand makes this possibility seem less likely because it would involve the rearrangement of several interstrand hydrogen bonds and a change in the orientations of the side chains near the bulge with respect to the sheet.

A more attractive candidate for the slowly interconverting native conformers is the cis peptide bond between Gly-95 and Gly-96 at the end of strand βE. X-ray structures of various liganded states of DHFR show that this bond is a mixture of the cis and trans isomers in apoDHFR (Bystroff & Kraut, 1991) and is entirely in the cis form in the ternary complex with folate and $NADP^+$ (Bystroff *et al.*, 1990). The cis isomer is required in the ternary complex to allow cofactor binding. This proposal is consistent with the observation that $NADP^+$ can only bind in one of the two folding channels in C85S/

C152E DHFR. Replacement of Gly-95 with a side chain that contains a β-carbon would strongly disfavor the cis isomer and, therefore, would provide a test of this hypothesis (Villafranca *et al.*, 1983). Such experiments are in progress.

The observation that the number of folding channels in DHFR can be reduced by the replacement of Cys-85 with serine has two important implications: (1) At least one source of conformational heterogeneity in protein folding reactions can be alternative tertiary structures. In the case of DHFR, some of these alternative conformers appear to reflect different orientations of a pair of structural domains. (2) The simplification of the kinetic mechanism of folding enhances the ability to treat quantitatively the effects of other mutations on the various intermediates which appear along the folding pathway. The reduction in complexity should also simplify the analysis of pulse-labeling NMR experiments (Englander & Mayne, 1992; Baldwin & Roder, 1991) which would monitor the formation of the hydrogen-bonding network in DHFR.

ACKNOWLEDGMENT

We thank Drs. Patricia Jennings, Craig J. Mann, and Jill A. Zitzewitz for critical reading of the manuscript and helpful discussion, Dr. Bryan Finn for sharing his unpublished results, and Gregory Lazar for retrieving many references from the literature.

REFERENCES

Alonso, D. O. V., & Dill, K. A. (1991) *Biochemistry 30*, 5974–5985.
Appleman, J. R., Howell, E. E., Kraut, J., Kühl, M., & Blakley, R. L. (1988) *J. Biol. Chem. 263*, 9187–9198.
Baldwin, R. L. (1975) *Annu. Rev. Biochem. 44*, 453–475.
Baldwin, R. L., & Roder, H. (1991) *Curr. Opin. Struct. Biol. 1*, 218–220.
Bitar, K. G., Blankenship, D. T., Walsh, K. A., Dunlap, R. B., Reddy, A. V., & Freisheim, J. H. (1977) *FEBS Lett. 80*, 119–122.
Bolin, J. T., Filman, D. J., Matthews, D. A., Hamlin, R. C., & Kraut, J. (1982) *J. Biol. Chem. 257*, 13650–13662.
Bradford, M. M. (1976) *Anal. Biochem. 72*, 248–254.
Brandts, J. F., Halvorson, H. R., & Brennan, M. (1975) *Biochemistry 14*, 4953–4963.
Bystroff, C., & Kraut, J. (1991) *Biochemistry 30*, 2227–2239.
Bystroff, C., Oatley, S. J., & Kraut, J. (1990) *Biochemistry 29*, 3263–3277.
Chen, B.-L., Baase, W. A., & Schellman, J. A. (1989) *Biochemistry 28*, 691–699.
Elöve, G. A., & Roder, H. (1991) *ACS Symp. Ser. 470*, 50–63.
Englander, S. W., & Mayne, L. (1992) *Annu. Rev. Biophys. Biomol. Struct. 21*, 243–265.
Evans, P. A., Kautz, R. A., Fox, R. O., & Dobson, C. M. (1989) *Biochemistry 28*, 362–370.
Falzone, C. J., Benkovic, S. J., & Wright, P. E. (1990) *Biochemistry 29*, 9667–9677.
Falzone, C. J., Wright, P. E., & Benkovic, S. J. (1991) *Biochemistry 30*, 2184–2191.
Frieden, C. (1990) *Proc. Natl. Acad. Sci. U.S.A. 87*, 4413–4416.
Gleisner, J. M., Peterson, D. L., & Blakley, R. L. (1974) *Proc. Natl. Acad. Sci. U.S.A. 71*, 3001–3005.
Hillcoat, B. L., Nixon, P. F., & Blakley, R. L. (1967) *Anal. Biochem. 21*, 178–189.
Iwakura, M., Kawata, M., Tsuda, K., & Tanaka, T. (1988) *Gene 64*, 9–20.
Iwakura, M., Furusawa, K., Kokubu, T., Ohashi, S., Tanaka, Y., Shimura, Y., & Tsuda, K. (1992) *J. Biochem. (Tokyo) 111*, 37–45.
Jennings, P. A., Finn, B. E., Jones, B. E., & Matthews, C. R. (1993) *Biochemistry 32*, 3783–3789.
Kiefhaber, T., Grunert, H.-P., Hahn, U., & Schmid, F. X. (1992) *Proteins: Struct., Funct., Genet. 12*, 171–179.
Kuwajima, K., Mitani, M., & Sugai, S. (1989) *J. Mol. Biol. 206*, 547–561.
Kuwajima, K., Garvey, E. P., Finn, B. E., Matthews, C. R., & Sugai, S. (1991) *Biochemistry 30*, 7693–7703.
Laemmli, U. K. (1970) *Nature 227*, 680–685.
Matthews, C. R. (1987) *Methods Enzymol. 154*, 498–511.
Mullins, L. S., Pace, C. N., & Raushel, F. M. (1993) *Biochemistry 32*, 6152–6156.
Radford, S. E., Dobson, C. M., Evans, P. A. (1992) *Nature 358*, 302–307.
Rance, M., Sørensen, O. W., Bodenhausen, G., Wagner, G., Ernst, R. R., & Wüthrich, K. (1983) *Biochem. Biophys. Res. Commun. 117*, 479–485.
Santoro, M. M., & Bolen, D. W. (1988) *Biochemistry 27*, 8063–8068.
Schellman, J. A. (1978) *Biopolymers 17*, 1305–1322.
Schmid, F. X. (1983) *Biochemistry 22*, 4690–4696.
Stone, S. R., Montgomery, J. A., & Morrison, J. F. (1984) *Biochem. Pharmacol. 33*, 175–179.
Tanford, C. (1968) *Adv. Protein Chem. 23*, 122–275.
Tonomura, B., Nakatani, H., Ohnishi, M., Yamaguchi-Ito, J., & Hiromi, K. (1978) *Anal. Biochem. 84*, 370–383.
Touchette, N. A., Perry, K. M., & Matthews, C. R. (1986) *Biochemistry 25*, 5445–5452.
Villafranca, J. E., Howell, E. E., Voet, D. H., Strobel, M. S., Ogden, R. C., Abelson, J. N., & Kraut, J. (1983) *Science 222*, 782–788.
Weissman, J. S., & Kim, P. S. (1991) *Science 253*, 1386–1393.